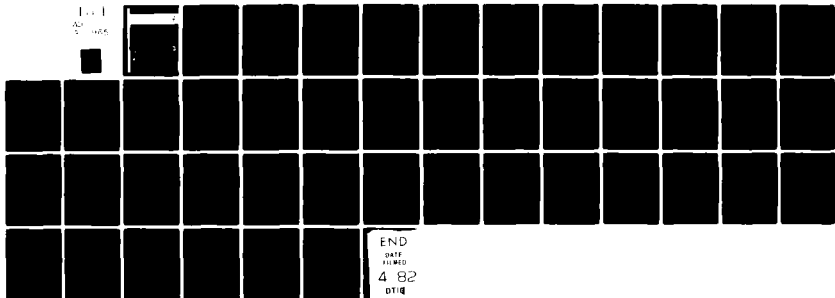


AD-A111 965

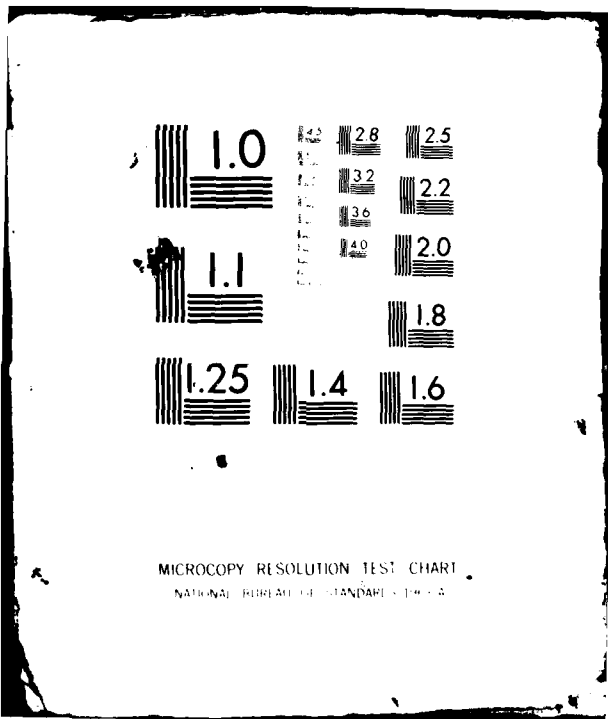
TECHNION - ISRAEL INST OF TECH HAIFA DEPT OF AERONAU--ETC F/6 11/6
SEMI INEXTENSIONAL POST BUCKLING ANALYSIS OF ANNULAR PLATES, (U)
SEP 81 A LIBAI AFOSR-81-0016
TAE-466 NL

UNCLASSIFIED

1-1
AD 466



END
DATE
FILMED
4 82
DTIC



MICROCOPY RESOLUTION TEST CHART
NATIONAL BUREAU OF STANDARDS-1963-A

①

September 1981

TAE No. 466

Semi Inextensional Post Buckling Analysis of Annular Plates

by

A. Libai

DTIC
ELECTE
MR 12 1982
S D

Scientific Report No. 2

Approved for public release; distribution unlimited.

Report for
Structural and Dynamic Division, Air Force Wright Aeronautical Laboratories
and
European Office of Aerospace Research and Development, Dayton, Ohio

ADA 111 965

FILE COPY

September 1981

SEMI-INEXTENSIONAL POST BUCKLING ANALYSIS
OF ANNULAR PLATES

by

A. Libai

Department of Aeronautical Engineering
Technion - Israel Institute of Technology
Haifa, Israel

TAE No. 466

The research reported in this document has been sponsored in part by
the Air Force Office of Scientific Research. United Air Force Contract
AFOSR-81-0016.

Distribution of this document is unlimited.

ABSTRACT

The field equation for meridionally inextensional axisymmetric deformations of shells of revolution is developed and applied to the postbuckling analysis of simply-supported imperfect annular plates subjected to compressive edge loads. The semi-inextensional model is then compared with the usual extensional model by using an energy approach with two and three deformation parameters.

The method is used to analyse the postbuckling behavior of an imperfect annular plate with an eccentric interior edge stiffener. The results show that although either imperfection or eccentricity lead to stable behavior, their combination may introduce unstable imperfection-sensitive behavior in some cases.

-1-

Accession For	
NTIS CHAS1	<input checked="" type="checkbox"/>
DTIC TAB	
Unannounced	
Justification	
By	
Distribution/	
Availability Codes	
Avail and/or	
Special	
DIST	
A	



TABLE OF CONTENTS

Abstract

Table of Contents

1. Introduction
2. Plate Model, Geometry and Kinematics
3. Equilibrium Equations
4. Constitutive Laws
5. Approximations
6. Semi-Inextensional Axisymmetric Shell and
Plate Analysis
7. Three-Parameter Extensional Model
8. Radially Inextensional Model with an Eccentrically
Reinforced Edge
9. Buckling, Post Buckling and Sensitivity of Eccentrically
Stiffened Imperfect Annular Plates
10. Summary of Results

Appendix: Equations for a Three-Parameter Semi-Inextensional
Model

References

List of Figures

1. INTRODUCTION

The postbuckling deformations of many plates and shells exhibit rather large rotations and curvature changes while the midsurface extensional strains have a rather limited influence on the deformation patterns. This type of behavior is related to the so-called "small-strain-finite-rotation" theory of plates and shells which assumes that the equations can be linearized in the extensional strains but not in the rotations (and displacements).

In many practical applications it has been observed that the incremental extensional strains during the post-buckling deformation process are sufficiently small and over most of the shell (or plate) so that the deformation could presumably be approximated by an inextensional model which eliminates the incremental extensions completely. However, attempts to do so have been found to be not entirely satisfactory because of two main reasons:

(a) The need for the existence of localised regions of high strain gradients in order to account for the boundary conditions and for the internal compatibility of the shell deformation pattern. A good example is the diamond pattern of the buckled very thin cylindrical shell which requires significant strain gradients along its creases and corners where the Gaussian Curvature of the surface undergoes large changes.

(b) In some cases the inextensional deformation has a definite *directional pattern*. That is, the incremental deformations are virtually inextensional in one direction at each point, while having a substantial extensional component in the direction orthogonal to it. Quite a few

postbuckling patterns possess this property. To cite a few examples, the strong postbuckling of thin plates in shear, of thin shells of revolution in twist, of cylindrical shells and of annular plates in axisymmetric compression, are all of this type.

For the latter class of structures, semi-inextensional models can be postulated. By doing so, the postbuckling analysis can be simplified both by decreasing the number of variables and by a priori taking into account the observed deformation patterns. In some other cases, a combination of semi-inextensionality plus localised areas of high strain gradients may be useful.

Some of the features of semi-inextensional plate models will be exemplified in this study by considering the axisymmetric postbuckling behavior of an imperfect annular plate. In addition, the study will include an examination of the interaction of shape imperfections and boundary eccentricities. This might be of some use to the understanding of this complex phenomenon in more complicated structures.

The problem of the axisymmetric postbuckling behavior of annular plates has been considered in the past by several investigators [7,9,10,11,12,15] with the clamped external boundary being the more popular case. Treatment consisted of solving the axisymmetric Von-Karman plate equations by using either series expansion techniques or especially devised numerical methods. In recent years, general and special purpose computer codes were utilised too. These methods have their advantages in accuracy but suffer from the drawback of being difficult to use for overall design data or for the evaluation of trends.

The approximate analytical approach presented here for the evaluation of simply supported annular plates under compressive edge loads is based on experimental observations both for its basic assumption of radial inextensionality and for its choice of deformation model. The semi-inextensionality assumption is used for deriving the differential equation for the large rotations of shells and annular plates, whereas the deformation model is combined with an energy approach to produce a simple approximate model of post-buckling behavior. It is believed that this and similar approaches are suitable for engineering estimates and as necessary adjuncts to testing programs.

Observations made during a recent testing program [8,p.19; 10] on simply supported annular plates have demonstrated that as high post-buckling loads were reached, plates with free internal edges or with weak rings tended to deform into shapes which were close to shallow cones. Marked deviations appeared only if the stiffening rings at the interior edge were relatively heavy. A similar mode of behavior- although with a different loading case - was noted in the study of shallow conical springs by Almen and Laszlo in 1936 and later by Wempner [2] and by Schmidt and Wempner [3]. This observation will be subsequently used in the determination of the initial deformation model.

2. PLATE MODEL, GEOMETRY AND KINEMATICS

Let (r, z, θ) be a cylindrical coordinate system in space, to which an annular plate or shell is referred (see Fig. 1). The interior boundary of the plate ($r=b$) may be stiffened by an eccentric ring. Compressive radial forces P (per unit length) are applied to the exterior boundary ($r=a$).

The initial configuration of the imperfect plate is that of a very shallow shell of revolution, with $\phi_0(r)$ being the angle between the normal to the surface and the positive direction of the z axis. (Note: the magnitude of ϕ_0 in Fig. 1 is exaggerated.) Length measure along the plate midsurface in the r - z plane is denoted by s and its local radius of curvature by r_ϕ . Obviously, the following two relationships hold:

$$\frac{1}{r_\phi} = \frac{d\phi_0}{ds} \quad \text{and} \quad dr = \cos\phi_0 ds \quad (1)$$

The plate deforms from its initial configuration into another shell of revolution with length measure s' . The radial displacement of a material point on the plate midsurface is denoted by u (Fig. 2). The angle between the normal to the deformed plate and the z axis is denoted by ϕ , and the radius of curvature of the deformed plate midsurface is r'_ϕ . The following relationships hold:

$$\frac{1}{r'_\phi} = \frac{d\phi}{ds'} \quad dr' = \cos\phi ds'$$

Note that primes relate to the deformed configuration (except for ϕ which is measured in the deformed configuration).

An expression for the meridional strain ϵ_r can be derived directly from Fig. 2:

$$ds' \cos \phi = ds \cos \phi_0 + du$$

or, in view of (1):

$$\epsilon_r = \left(1 + \frac{du}{dr}\right) \frac{\cos \phi_0}{\cos \phi} - 1 \quad (2)$$

See also equation (15) in Ref. [1].

The radial displacement can be calculated from (2) as follows:

$$u = \int [(1 + \epsilon_r) \cos \phi - \cos \phi_0] ds + u_0 \quad (3)$$

The circumferential strain ϵ_ϕ is obtained directly from its definition

$$\epsilon_\phi = u/r \quad (4)$$

These also lead to the strain compatibility equation:

$$(1 + \epsilon_r) \cos \phi - \cos \phi_0 = \frac{d}{ds}(r \epsilon_\phi) \quad (5)$$

Bending strains should be derived in principle from the usual Kirchoff-Love assumptions of transversely rigid shells. There is no final agreement on the "proper" form to be used. Strict application of the K.L. hypothesis leads to a formula of the type:

$$K^* = (1 + \epsilon) \left(\frac{1}{R'} - \frac{1}{R} \right) \quad (6a)$$

Here ϵ is an extensional strain and R is a radius of curvature.

On the other hand, an alternate definition

$$K = (1 + \epsilon) \frac{1}{R'} - \frac{1}{R} \quad (6b)$$

is widely used. It has also been shown to have a wide range of validity in small and large strain analysis [14, p. 94]. Their difference is the quantity ϵ/R . Fortunately, in this study the strains are small and, moreover, the imperfect undeformed plate is almost flat so that R is very large. Hence, the difference is quite negligible, and the second definition will be adopted for convenience. This leads to the following expressions for the bending strains:

$$K_r = \frac{ds'}{ds} \left(\frac{d\phi}{ds'} \right) - \frac{d\phi_0}{ds} = \frac{d}{ds} (\phi - \phi_0) \quad (7)$$

$$K_\theta = \frac{r+u}{r} \left(\frac{\sin\phi}{r+u} \right) - \frac{\sin\phi_0}{r} = \frac{1}{r} (\sin\phi - \sin\phi_0) \quad (8)$$

This is also the form adopted (as an approximation!) by Reissner in his nonlinear theory of shells of revolution [1, eqns. 17,18].

From equations (3), (4), (7), (8) it follows that all the extensional and bending strains have been expressed in terms ϵ_r , ϕ and the constant of integration u_0 .

3. EQUILIBRIUM EQUATIONS

Equilibrium is considered in the deformed (prime) configuration. The force resultant vector acting on the cross section $r' = c$ can be decomposed into either tangential (N'_r) and transverse (Q') or radial (H') and axial (V') resultants respectively. These are related by the equations (see Fig. 2):

$$V' = N'_r \sin\phi + Q' \cos\phi \quad (9)$$

$$H' = N'_r \cos\phi - Q' \sin\phi \quad (10)$$

Axial equilibrium requires that $V' = 0$, so that N'_r can be expressed in terms of Q' as follows:

$$N'_r = -Q' \cot\phi \quad (11)$$

The second equilibrium equation is in the radial direction and yields the expression:

$$\frac{d}{ds'} (H' r') = N'_\theta$$

Now, H' can be eliminated from the equations by using the expression for N'_r and substituting:

$$H' = -Q' \cot\phi \cos\phi - Q' \sin\phi = -\frac{Q'}{\sin\phi}$$

so that the equilibrium equation becomes

$$\frac{d}{ds'} \left(\frac{Q' r'}{\sin\phi} \right) + N'_\theta = 0 \quad (12)$$

In many applications stress resultants defined per units of length of the undeformed shell cross sections are of advantage, especially in conjunction with constitutive laws. These are defined by:

$$Q = \frac{r'}{r} Q' ; N_r = \frac{r'}{r} N'_r ; M_r = \frac{r'}{r} M'_r ; N_\theta = \frac{ds'}{ds} N'_\theta ; M_\theta = \frac{ds'}{ds} M'_\theta$$

Then the force equilibrium equation reduces to

$$\frac{d}{ds} \left(\frac{Qr}{\sin\phi} \right) + N_\theta = 0 \quad (13)$$

The equation of moment equilibrium in the prime configuration is that of a shell of revolution:

$$\frac{d}{d\phi} (r'M'_r) - M'_\theta r'_\phi \cos\phi = r'r'_\phi Q'$$

or:

$$\frac{d}{ds} (rM'_r) - M'_\theta \cos\phi = r'Q'$$

Passing again to the stress resultants per unit undeformed length, the following results:

$$\frac{d}{ds} (rM_r) - M_\theta \cos\phi = \frac{ds'}{ds} rQ = (1+\epsilon_r) rQ \quad (14)$$

Hence, all the equations of equilibrium are reducible to the single equation:

$$\frac{d}{ds} \left[\frac{\frac{d}{ds} (rM_r) - \cos\phi M_\theta}{(1+\epsilon_r) \sin\phi} \right] + N_\theta = 0 \quad (15)$$

Note that all the variables are measured now with respect to the geometry of the undeformed configuration.

4. CONSTITUTIVE LAWS

It will be assumed that the stress resultants per unit undeformed length are related to the strain measures by the usual Hooke's law. This, plus the other assumptions of the Kirchhoff-Love hypothesis lead to the commonly used constitutive laws of plate and shell theory:

$$\begin{aligned}
 M_r &= -D(K_r + \nu K_\theta) = -\frac{\partial W}{\partial K_r} \\
 M_\theta &= -D(K_\theta + \nu K_r) = -\frac{\partial W}{\partial K_\theta} \\
 N_r &= C(\epsilon_r + \nu \epsilon_\theta) = \frac{\partial W}{\partial \epsilon_r} \\
 N_\theta &= C(\epsilon_\theta + \nu \epsilon_r) = \frac{\partial W}{\partial \epsilon_\theta}
 \end{aligned}
 \tag{16}$$

with

$$C = \frac{Eh}{1-\nu^2} \quad ; \quad D = \frac{Eh^3}{12(1-\nu^2)} = \frac{h^2}{12} C$$

The strain energy function, per unit area of the undeformed reference surface is also given in its common separated form

$$W = \frac{C}{2}(\epsilon_r^2 + \epsilon_\theta^2 + 2\nu\epsilon_r\epsilon_\theta) + \frac{D}{2}(K_r^2 + K_\theta^2 + 2\nu K_r K_\theta)
 \tag{17}$$

Here the shear terms have been deleted because of the axisymmetry. Regarding the magnitudes of the strains, equation (17) should be valid for the same range of (small) strains for which Hooke's Law is valid. For larger strains, more refined forms for the strain energy (or else, other constitutive laws) ought to be used.

5. APPROXIMATIONS (GENERAL CONSIDERATIONS)

There are several approximations and simplifications to the nonlinear expressions obtained above. These are related, as is usual in plate and shell theory, to four distinct properties of any given shell problem:

- (a) Constitutive laws and the magnitude of the strains. Here, the small strain approximation, which is usually made, is valid for most engineering materials in the elastic (and low plastic) range.
- (b) Particular geometry. Here, it may be assumed that the initial imperfection ϕ_0 is sufficiently small so that the approximation $dr \approx ds$ can be (carefully!) introduced where appropriate.
- (c) Restrictions on the magnitude of the rotation. Here, the quadratic approximation can be introduced for $\cos\phi$ (to within 0.4% for $\phi \leq 30^\circ$) and the linear (to within 4.5% for $\phi \leq 30^\circ$) or cubic (to within .07% for $\phi \leq 30^\circ$). approximations introduced for $\sin\phi$.
- (d) Assumptions based on the estimated mode of behavior. Here, the semi-inextensional approximation may be introduced by taking $\epsilon_r \rightarrow 0$. This assumption must be justified by ~~aposteriori~~ comparisons with more complete solutions or with experimental observations. It should be noted here, though, that this is not the only possible approximation. For example, the methods of references four and thirteen which omit or replace terms in the elastic strain energy function have been used with a varying amount of success for the study of the large deflection of plates.

The present study makes selective use of the first three approximations, with the intention of developing and examining the fourth, e.g. the semi-inextensional assumption.

Some examples of the uses of approximations (a), (b) and (c) are as follows:

Using assumption (b) and (c), the expression for u becomes

$$u = \int [(1 + \epsilon_r) \cos \phi - \cos \phi_0] dr = \int [(1 - \frac{1}{2}\phi^2) \epsilon_r + \frac{1}{2}(\phi_0^2 - \phi^2)] dr + O(\phi^4) \quad (3a)$$

The expression for ϵ_r in terms of u and ϕ is:

$$\epsilon_r = (1 + \frac{du}{dr}) \cos \phi_0 \sec \phi - 1 = \frac{du}{dr} + \frac{1}{2}(\phi^2 - \phi_0^2) + \dots \quad (2a)$$

whereas the compatibility equation reduces to:

$$\frac{d}{dr}(r\epsilon_\theta) = (1 - \frac{1}{2}\phi^2) \epsilon_r + \frac{1}{2}(\phi_0^2 - \phi^2) + O(\phi^4) \quad (5a)$$

Using (a) and (b), the expression for the meridional bending strain is:

$$K_r = \frac{d}{dr}(\phi - \phi_0) \quad (7a)$$

Using (a) and (b), the curvature compatibility equation reduces to:

$$\frac{d}{dr}(rK_\theta) = \cos \phi K_r$$

Introduction of the quadratic approximation (c) for $\cos \phi$ yields further:

$$\frac{d}{dr}(rK_\theta) = (1 - \frac{1}{2}\phi^2) K_r + O(\phi^5)$$

This equation is of the same order of accuracy as the cubic approximation for K , together with (b):

$$rK_\theta = (\phi - \phi_0) - \frac{1}{6}(\phi^3 - \phi_0^3) + O(\phi^5) \quad (8a)$$

For most purposes the linear approximation is sufficient:

$$rK_\theta = \phi - \phi_0 + O(\phi^3) \quad (8b)$$

so that:

$$\frac{d}{dr}(rK_\theta) = K_r$$

6. SEMI-INEXTENSIONAL AXISYMMETRIC SHELL AND PLATE ANALYSIS

In this model, the radial strains are omitted in the shell analysis in comparison with the circumferential strains and the rotations (whose magnitudes are not restricted).

Differentiation of the equilibrium equation (15) while making use of (2), (4) and (16), and putting $\epsilon_r = 0$ throughout, yields the expression:

$$\frac{d}{ds} \left\{ r \frac{d}{ds} \left[\frac{\frac{d}{ds}(rM_r) - \cos\phi M_\phi}{\sin\phi} \right] \right\} + C(\cos\phi - \cos\phi_0) = 0$$

Making further use of (16) and also of (7) and (8) leads to a fourth order differential equation in ϕ :

$$\frac{d}{ds} \left\{ \left[r \frac{d}{ds} \left\{ \frac{1}{\sin\phi} \left[\frac{d}{ds} \left(r \frac{d\phi}{ds} - r \frac{d\phi_0}{ds} \right) - \frac{\cos\phi}{r} (\sin\phi - \sin\phi_0) + \sqrt{\frac{d\phi_0}{ds}} (\cos\phi - \cos\phi_0) \right] \right\} \right] \right\} - \frac{12}{h^2} (\cos\phi - \cos\phi_0) = 0$$

Noting that for thin plates and shells $\frac{12}{h^2} \gg 1$, the omission of the term with $\sqrt{\frac{d\phi_0}{ds}}$ in comparison with the last term is justified, yielding the simplified form:

$$\frac{d}{ds} \left\{ \left[r \frac{d}{ds} \left\{ \frac{1}{\sin\phi} \left[\frac{d}{ds} (\phi - \phi_0) \right] - \frac{\cot\phi}{r} (\sin\phi - \sin\phi_0) \right\} \right] \right\} - \frac{12}{h^2} (\cos\phi - \cos\phi_0) = 0$$

(18)

The last equation describes the axisymmetric semi-inextensional deformations of shells of revolution in general. The input into the equation is the initial shape $[r(s) \text{ and } \phi_0(s)]$ and appropriate boundary conditions. The result would be $\phi(s)$ which expresses the angular coordinate of the deformed shell in terms of the Lagrangian variable s . The other terms which complete the description of the deformed configuration are

$$u = \int (\cos\phi - \cos\phi_0) ds$$

$$v = \int (\sin\phi - \sin\phi_0) ds$$

where u and v are the radial and axial displacements respectively. The bending strains $(K_r; K_\theta)$ and extensional strain ϵ_θ can then be calculated from (7), (8) and (4), thus facilitating the calculation of the moments $(M_r; M_\theta)$, force resultant N_θ , and shearing force Q_r . The meridional stress resultant N_r can be calculated from:

$$N_r = - Q_r \cot\phi$$

(The constitutive laws cannot be applied for the calculation of N_r because of the meridional inextensionality assumption). Note that for $\phi = 0$, N_r cannot be calculated in a direct fashion because of the apparent singularity, but $\lim_{\phi \rightarrow 0} N_r$ does exist, as will be seen later

The imperfect annular plate is included in the broader class of "shallow initial configurations" defined by approximation (b). Replacing ds with dr , the result is:

$$\frac{d}{dr} \left\{ r \frac{d}{dr} \left\{ \frac{1}{\sin \phi} \frac{d}{dr} \left[r \frac{d}{dr} (\phi - \phi_0) \right] - \frac{\cot}{r} (\sin \phi - \sin \phi_0) \right\} \right\} -$$

$$- \frac{12}{h^2} (\cos \phi - \cos \phi_0) = 0 \quad (19)$$

Here, also, the following can be used (if desired):

$$\sin \phi_0 \approx \phi_0$$

$$\cos \phi_0 \approx 1 - \frac{1}{2} \phi_0^2 \approx 1$$

The latter approximations do not lead to any obvious advantage unless the deformed configuration is shallow too, in which case an expansion of the trigonometric terms up to quadratic (or cubic) terms in ϕ would make the equation more "manageable" from a mathematical point of view. In such a case, the use of a new variable

$$\beta = \phi - \phi_0$$

and expansions in β may be of advantage.

Equations (18) and (19) can be cast into algebraic forms by using the new variable $y = \sin \phi$. Then:

$$\cos \phi = (1 - y^2)^{\frac{1}{2}}$$

$$\frac{d\phi}{ds} = (1 - y^2)^{\frac{1}{2}} \frac{dy}{ds}$$

$$\cot \phi = y^{-1} (1 - y^2)^{\frac{1}{2}}$$

and so forth. This form is particularly suited to uses of the equations in conjunction with standard numerical programs for solving ordinary differential equations.

Methodology:

While further analysis of the semi-inextensional differential equation may be rewarding in itself, the purpose of comparing this model with the more complete (and more complex) extensional model, can be achieved by far simpler means which should offer their own rewards.

At the first stage of the investigation, simple deformation patterns will be used in order to compare the regular plate model (which includes the effects of ϵ_p) with the semi-inextensional model. The theorem of the minimum of the total potential will be utilized to obtain the response of the plate to compressive edge forces within the assumed deformation modes. At this stage the inner edge of the plate will be free. The initial imperfection of the plate will be in the form of a very shallow cone with a constant ϕ_0 . The fact that this is actually the governing imperfection of the simply supported annular plate has been borne out by experiments [8, Figs. 9b, 17a, 17b].

The comparison between the two models should provide an indication of the adequacy of the semi-inextensional model, since a three parameter extensional model will be compared with a two parameter semi-inextensional model. The comparison will concentrate on the region of the buckling point itself. The reason is that the semi-inextensional model should have its greatest difficulties and inaccuracies as $\phi, \phi_0 \rightarrow 0$.

A three parameter more complex semi-inextensional model will also be presented (see Appendix). It will not be investigated in detail since it has been argued that only the simplest nontrivial models should be investigated by analytical tools and more complex models are, in many cases, inferior to direct numerical procedures. This point is left open.

At the next stage, the effects of an interior edge beam will be incorporated into the semi-inextensional analysis. This should facilitate the study of the comparative roles and interactions of the edge beam eccentricity e and the initial imperfection ϕ_0 . The possibility that the interaction can cause essential changes in the response will be looked into. The fact that an eccentrically stiffened imperfect plate can be imperfection sensitive has been verified experimentally.

7. Three-Parameter Extensional Model

Consider a displacement field of the form:

$$\begin{aligned}u &= u_0 + ru_1 \\ \phi &= \phi_1 - \phi_0\end{aligned}\tag{20}$$

where ϕ_0 is the initial imperfection and u_0 ; u_1 ; ϕ_1 are constant deformation parameters to be determined by minimizing the total potential. The deformation pattern assumes that the dominant post-buckling mode is that of a shallow cone. This has been well-correlated with experiments on annular plates [8, p. 19 and figs. 9b, 17a, 17b]. Using the quadratic approximations for the various strain measures and applying equations (2a), (4), (7), (8b), the following expressions result:

$$\epsilon_r = u_1 + \frac{1}{2}(\phi_1^2 - \phi_0^2)$$

$$\epsilon_\theta = \frac{1}{r} u_0 + u_1$$

Also:

$$K_r = 0$$

$$K_\theta = \frac{1}{r}(\phi_1 - \phi_0)$$

The total elastic potential of the system is:

$$V = \pi D \int_b^a (K_r^2 + K_\theta^2 + 2\nu K_r K_\theta) r dr + \pi C \int_b^a (\epsilon_r^2 + \epsilon_\theta^2 + 2\nu \epsilon_r \epsilon_\theta) r dr + 2\pi a P u_a \quad (21)$$

where $u_a = u(r=a)$ and P is positive in compression.

Introducing the values of ϵ_r ; ϵ_θ ; K_r ; K_θ , the result for V is:

$$\begin{aligned} V = & \pi D (\phi_1 - \phi_0)^2 \ln(a/b) + \pi C \left\{ \frac{1}{2} (a^2 - b^2) \left[u_1 + \frac{1}{2} (\phi_1^2 - \phi_0^2) \right]^2 + [u_0^2 \ln(a/b) + \right. \\ & \left. + 2u_0 u_1 (a-b) + \frac{1}{2} u_1^2 (a^2 - b^2) \right] + 2\nu \left[u_1 + \frac{1}{2} (\phi_1^2 - \phi_0^2) \right] \left[u_0 (a-b) + \frac{1}{2} u_1 (a^2 - b^2) \right] \right\} \\ & + 2\pi a P (u_0 + a u_1) \quad (22) \end{aligned}$$

The total potential can be now minimized with respect to the parameters u_0 , u_1 , ϕ_1 , leading to three simultaneous equations in the parameters. These can be brought, after some manipulations and an elimination process, to the following cubic equation for ϕ_1 :

$$\lambda \bar{\phi}_1 = g_1 (\bar{\phi}_1 - \bar{\phi}_0) - g_2 (\bar{\phi}_1^2 - \bar{\phi}_0^2) \bar{\phi}_1 \quad (23)$$

where the loading parameter λ and modified rotations $\bar{\phi}_1$ are given by:

$$\lambda = \frac{P a^2}{D} \quad \bar{\phi}_1 = \frac{a}{h} \phi_1$$

Also:

$$g_1 = g_1(\mu) = \frac{-2[(1+\mu)\ell n\mu + (1+\nu)(1-\mu)]\ell n\mu}{1-\mu^2 + \nu(1-\mu)^2 + (1+\mu)\ell n\mu}$$

$$g_2(\mu) = \frac{-6(1-\nu)(1-\mu^2)[1-\mu + \frac{1}{2}(1+\mu)\ell n\mu]}{1-\mu^2 + \nu(1-\mu)^2 + (1+\mu)\ell n\mu}$$

$$\mu = b/a$$

For a given loading λ , geometrical ratio μ and imperfection $\bar{\phi}_0$, the equation can be easily solved for $\bar{\phi}_1$. Once $\bar{\phi}_1$ is known, the displacement parameters u_0 and u_1 can be easily calculated. These are given by:

$$\bar{u}_0 = g_3(\bar{\phi}_1^2 - \bar{\phi}_0^2) + g_4\lambda \quad (24)$$

$$\bar{u}_1 = g_5(\bar{\phi}_1^2 - \bar{\phi}_0^2) + g_6\lambda \quad (25)$$

where:

$$g_3 = \frac{1}{4\Delta} (1-\nu)(1-\mu^2)$$

$$g_4 = -\frac{\mu}{12\Delta}$$

$$g_5 = \frac{1}{\Delta} \left[\frac{1}{2}\nu(1-\mu) + \frac{1}{4}(1+\mu)\ell n\mu \right]$$

$$g_6 = \frac{1}{12\Delta} \left[1 + \frac{\ell n\mu}{(1-\mu)(1+\nu)} \right]$$

$$\Delta = - (1+\mu)\ell n\mu - (1+\nu)(1-\mu)$$

$$\bar{u}_i = \frac{a}{h^2} u_i$$

The special case $\bar{\phi}_0 = 0$ is that of the perfect plate. The equation for $\bar{\phi}_1$ breaks down into the straight line $\bar{\phi}_1 = 0$ which describes the prebuckling behavior and the parabolic "equilibrium path":

$$\lambda = g_1 - g_2 \phi_1^2$$

which describes the postbuckling behavior of the plate. The intersection is at

$$\lambda = \lambda_{cr} = g_1$$

where λ_{cr} is the critical (buckling) loading parameter. The equilibrium paths of the imperfect plate are cubic parabolas. These parabolas approach the two curve system of the perfect plate as $\bar{\phi}_0 \rightarrow 0$. Also, for a given ϕ_0 , the two curves approach each other for $\bar{\phi}_1 \gg \bar{\phi}_0$. This signifies the fact that for very large displacements the initial imperfection is not too important.

Considering now the radial displacements, it is convenient to refer to the displacement at a given point. The inner edge displacement $u_b = u(r=b)$ is chosen because of the direct connection between this displacement and the circumferential stress level at the inner edge. An expression for \bar{u}_b is:

$$\bar{u}_b = (g_3 + \mu g_5) (\bar{\phi}_1^2 - \bar{\phi}_0^2) + (g_4 + \mu g_6) \lambda \quad (26)$$

Another expression can be obtained by eliminating $(\bar{\phi}_1^2 - \bar{\phi}_0^2)$ through the use of the equation of the cubic parabola. This yields:

$$\bar{u}_b = \frac{g_1}{g_2} (g_3 + \mu g_5) \left(\frac{\phi_1 - \phi_0}{\phi_1} \right) - \left(\frac{g_3 + \mu g_5}{g_2} - g_4 - \mu g_6 \right) \lambda \quad (27)$$

The equilibrium path of the perfect plate $\bar{\phi}_0 = 0$ consists of two straight lines: the prebuckling line

$$\bar{u}_b^1 = (g_4 + \mu g_6) \lambda$$

and the postbuckling line

$$\bar{u}_b^2 = \frac{g_1}{g_2} (g_3 + \mu g_5) - \left(\frac{g_3 + \mu g_5}{g_2} - g_4 - \mu g_6 \right) \lambda$$

The two lines intersect at the buckling point, where

$$u_b(\lambda = \lambda_{cr}) = u_{bc} = (g_4 + \mu g_6) g_1$$

Note that the radial motion reverses its direction at the buckling point. It is inward up to the point and outward thereafter.

Again, the equilibrium path of the imperfect plate provides a smooth transition between the pre- and post-buckling regions, approaching the straight line of the perfect plate for $\lambda \gg \lambda_{cr}$.

The fact that the high postbuckling curve of the plate approaches a straight line was observed experimentally [8], [10], where the use of the two asymptotic straight lines for the experimental determination of the critical load led to satisfactory results [10]. This agrees quite well with the results of this section and indicates that the three parameter model is sufficient to indicate the main features of the deformation process. As will be seen later, the model gives also surprisingly good quantitative predictions of the buckling point over a wide range of the geometrical parameter.

8. Radially Inextensional Model with an
Eccentrically Reinforced Edge

The condition of radial inextensionality imposes a relationship between the rotations and radial displacement. For a quadratic approximation of the cosine function the relationship is:

$$u = u_b - \frac{1}{2} \int_b^r (\phi^2 - \phi_o^2) dr \quad (28)$$

Hence:

$$\epsilon_\theta = \frac{1}{r} [u_b - \frac{1}{2} \int_b^r (\phi^2 - \phi_o^2) dr] \quad (29)$$

The expressions for K_r and K_θ in terms of the rotations remain as before (7a, 8b).

It is assumed that an eccentric ring with area A moment of inertia I and eccentricity e (with respect to the plate center line) is attached to the inner boundary of the plate at $r=b$. Positive eccentricity is defined such that positive rotations at $r=b$ would cause outward motion of the extreme fibers of the ring (Fig. 1). Under these conditions, the circumferential strain in the ring is given by:

$$\epsilon_{\theta R} = \frac{u}{r} = \frac{1}{b} [u_b + (\phi - \phi_o)_b z] \quad (30)$$

where z is the axial coordinate in the ring (positive in the e direction). The radial variations within the ring are omitted in the analysis, for simplicity.

The inclusion of the ring in the analysis, while not important for the comparison with the extensional model, offers the capability for investigating

the interaction of boundary eccentricities with geometrical imperfections and their combined effect on the post buckling behavior.

The total potential of the system of a radially inextensional annular ring with an eccentric stiffening ring along the interior boundary of the plate becomes:

$$\begin{aligned}
 V &= \pi C \int_b^a r \epsilon_\theta^2 dr + \pi D \int_b^a (K_\theta^2 + K_r^2 + 2\nu K_r K_\theta) r dr + \pi E b \int_A \epsilon_{\theta R}^2 dA + 2P\pi a u_a \\
 &= \pi C \int_b^a \frac{1}{r} \left[u_b - \frac{1}{2} \int_b^r (\phi^2 - \phi_0^2) dr \right]^2 dr + \pi D \int_b^a \left\{ \left[\frac{d}{dr} (\phi - \phi_0) \right]^2 + \frac{1}{2} (\phi - \phi_0)^2 + \right. \\
 &\quad \left. + \frac{\nu}{r} \frac{d}{dr} [(\phi - \phi_0)^2] \right\} r dr + \frac{\pi E}{b} \left\{ I (\phi - \phi_0)_b^2 + [u_b + (\phi - \phi_0)_b e]^2 A \right\} \\
 &\quad + 2\pi a P \left[u_b - \frac{1}{2} \int_b^a (\phi^2 - \phi_0^2) dr \right] \tag{31}
 \end{aligned}$$

Here A is the cross sectional area of the ring, and I is the moment of inertia with respect to a radial axis through its centroid.

sequel, ϕ_0 will be taken to be that of a shallow cone. This form of imperfection, as noted before, is common and has been observed experimentally.

(a) Two Parameter Model with a Free Edge

This is the simplest model possible. The deformed shape is also taken to be that of a shallow cone. It is similar to the three parameter model discussed above, but needs only two parameters for its description. The parameters are:

$$\phi = \phi_1 = \text{constant} \quad \text{and} \quad u_b. \tag{32}$$

Also, $I = A = 0$ are taken in the analysis for the free edge. The form of the strain energy simplifies to:

$$V = \pi C \int_b^a \frac{1}{r} [u_b - \frac{1}{2}(r-b)(\phi_1^2 - \phi_0^2)]^2 dr + \pi D \int_b^a \frac{1}{r} (\phi_1 - \phi_0)^2 dr + 2\pi a P [u_b - \frac{1}{2}(b-a)(\phi_1^2 - \phi_0^2)] \quad (33)$$

or

$$\frac{V}{\pi a^2 C} = -\nu n_p \left(\frac{u_b}{a}\right)^2 - (1-\nu+\nu n_p) \left(\frac{u_b}{a}\right) (\phi_1^2 - \phi_0^2) + \frac{1}{8}(3\nu^2 - 4\nu + 1 - 2\nu^2 n_p) (\phi_1^2 - \phi_0^2)^2 - \frac{h^2}{12a^2} n_p (\phi_1 - \phi_0)^2 + \frac{h^2}{6a^2} \lambda \left[\frac{u_b}{a} - \frac{1}{2}(1-\nu)(\phi_1^2 - \phi_0^2) \right] \quad (34)$$

The total potential can now be minimized with respect to (u_b/a) and ϕ_1 . This results in the following equations for $\bar{\phi}_1$ and \bar{u}_b :

$$\lambda \bar{\phi}_1 = f_1 (\bar{\phi}_1 - \bar{\phi}_0) - f_2 (\bar{\phi}_1^2 - \bar{\phi}_0^2) \bar{\phi}_1 \quad (35)$$

$$\bar{u}_b = f_3 (\bar{\phi}_1^2 - \bar{\phi}_0^2) + f_4 \lambda \quad (36)$$

where:

$$f_1 = \frac{(\lambda n_p)^2}{\nu - 1 - \lambda n_p}$$

$$f_2 = \frac{6(1-\nu)^2 + 3(1-\nu^2)\lambda n_p}{\nu - 1 - \lambda n_p}$$

$$f_3 = \frac{\nu - 1 - \lambda n_p}{2\lambda n_p}$$

$$f_4 = \frac{1}{12\lambda n_p}$$

An alternate expression for \bar{u}_b is obtained by eliminating $(\bar{\phi}_1^2 - \bar{\phi}_0^2)$:

$$\bar{u}_b = \frac{f_3 f_1}{f_2} \left(\frac{\phi_1 - \phi_0}{\phi_1} \right) - \left(\frac{f_3}{f_2} - f_4 \right) \lambda \quad (37)$$

The similarity in form between the 3 parameter extensional model and 2 parameter semi-inextensional model is self evident. Also obvious is the fact that the semi-inextensional model requires a smaller number of parameters for the same (rotational) mode shape than the extensional model. The rest of the analysis follows along the same lines of the 3 parameter model, with the "f" functions replacing the "g" functions and with g_5 and g_6 deleted. The buckling load is given by

$$\lambda_{cr} = t_1$$

The prebuckling line for the radial displacements in the perfect plate is

$$\bar{u}_b' = t_4 \lambda$$

and that of the postbuckling line is:

$$\bar{u}_b'' = \frac{t_1 t_3}{f_2} - \left(\frac{t_3}{f_2} - t_4 \right) \lambda$$

In Table 1, values of the buckling parameter λ_c are given using: (a) theoretical (exact) calculations (b) three-parameter extensional model and (c) two-parameter semi-inextensional model. Also given are the other coefficients of the postbuckling equilibrium paths.

Table 1: Comparative Values of λ_{cr} and Coefficients

μ	0.2	0.3	0.4	0.5	0.6
(a) λ_{theor}	3.55	3.11	2.77	2.45	2.30
(b) $\lambda_{ext}^{=g_1}$	3.68	3.10	2.75	2.51	2.35
(c) $\lambda_{inext}^{=f_1}$	3.20	2.88	2.65	2.49	2.35
(b) g_2	-.857	-.621	-.436	-.291	-.180
(c) f_2	-.982	-.688	-.471	-.309	-.187

The table shows that the extensional model gives somewhat better predictions for the buckling parameters for small μ . This difference disappears for increasing μ and both models yield very good predictions. Even for $\mu = 0.2$, which is a rather extreme case, P_{inext} is within 10% of the exact value.

From a theoretical point of view, the inextensional model is not expected to yield accurate results for $\phi \rightarrow 0$ since the in-plane extensions are dominant in this range of the deformation process - and these are not accurately described by the model. Accuracy is expected to improve with increasing ϕ . Hence, the good results near $\phi = 0$ are quite satisfying and are good indications of the overall capability of the model even at extreme cases.

(b) Two Parameter Model with an Eccentric Stiffening Ring

The relative success of the simpler semi-inextensional model in the case of the free inner boundary, makes it the model of choice for the more complex case of the eccentrically stiffened plate, where both imperfections

and eccentricity interact. It should be stated, though, that the use of a two parameter model restricts the analysis to relatively weak rings. The reason is that the ring provides some restraint against rotation for the inner edge. The rotational restraint of a heavy ring is sufficiently close to the clamped edge condition, so that the "cone approximation" cannot adequately represent the bent shape of the plate, and a minimum of three parameters would be needed. For the basic equations for this more complex analysis, see Appendix.

Introduction of the assumed deformation mode into the more complete form of the total potential and differentiation with respect to ϕ_1 and u_b , lead to the following equations:

$$(\bar{\phi}_1 - \bar{\phi}_0) [d_3 + d_6 e^2 + (3\bar{\phi}_1 + \bar{\phi}_0) \bar{e} d_2 + (\bar{\phi}_1 + \bar{\phi}_0) \bar{\phi}_1 d_4] = (\bar{e} + \bar{\phi}_1 d_5) \lambda \quad (38)$$

$$\bar{u}_b = \frac{1}{d_1} [-12(\bar{\phi}_1 - \bar{\phi}_0) \bar{e} + (\bar{\phi}_1^2 - \bar{\phi}_0^2) d_2 - \lambda] \quad (39)$$

where:

$$\bar{A} = \frac{A(1-\nu^2)}{bh}$$

$$\bar{e} = \frac{\bar{A}e}{h}$$

$$\bar{\phi} = \frac{a}{b} \phi$$

$$d_1 = \bar{A} - \epsilon n u$$

$$d_2 = 6(1-\mu + \mu \epsilon n u)$$

$$d_3 = (\bar{A} - \epsilon n u) d_1$$

$$d_4 = 3(3\mu^2 - 4\mu + 1 - 2\mu^2 \epsilon n u) d_1 - \frac{1}{6} d_2^2$$

$$d_5 = (1-\nu)(\bar{A}-1) - \ell n \nu$$

$$d_6 = - \frac{12 \ell n \nu}{\bar{A}}$$

$$\bar{I} = \frac{EI}{Db}$$

$$\bar{u}_b = \frac{a}{h^2} u_b$$

If $\bar{A} = \bar{I} = 0$ are introduced here, the equations for the free edge result. The effects of the ring are twofold: Increases in the area A and moment of inertia I of the ring cause a corresponding increase in the effective stiffness of the reinforced plate through their effects on the coefficients, especially, d_3 and d_1 . However, these do not lend to qualitative changes in the behavior of the plate. On the other hand, the addition of the eccentricity leads to the appearance of new terms in the equations. The combination of eccentricity and initial imperfection introduces new modes of behavior which did not exist in the centric plate. This will be studied in more detail in the sequel.

8. BUCKLING, POST BUCKLING AND SENSITIVITY OF ECCENTRICALLY STIFFENED, IMPERFECT ANNULAR PLATES.

The investigation is carried out based on the semi-inextensional model with two parameters, assuming axisymmetric behavior.

As is well known, the perfect annular plate has a stable initial post-buckling behavior and is not imperfection sensitive. The addition of either an eccentric stiffening ring or an initial imperfection does not change

the stability of the behavior of the plate. The structural problem, though, is changed in either case from a bifurcation problem plus postbuckling to that of a nonlinear behavior problem with the external compressive load increasing monotonously with the deformation.

However, the situation is changed when both imperfection and eccentricity occur simultaneously. It can be shown that for some values of the imperfection and eccentricity parameters, the structure can buckle (that is, it has a bifurcation point). Furthermore, this point is unstable and is imperfection sensitive for a limited value of the imperfections to one side of it. This mode of behavior should be anticipated if it is recalled that the eccentricity reduces the order of the nonlinearity from the cubic to the quadratic [11] and that structures with quadratic nonlinearities are usually imperfection-sensitive (the different behavior of frames from that of beams is a common example).

To examine this mode of behavior within the scope of the simplified model, it is convenient to rewrite the equations by introducing the variable β and "equivalent imperfection" ϵ as follows:

$$\beta = \bar{\phi}_1 - \bar{\phi}_0 \quad \epsilon = \bar{\phi}_0 + \frac{1}{d_5} \bar{e} \quad (40)$$

The equation for the equilibrium path $\lambda = \lambda(\beta)$ becomes then:

$$\lambda(\beta + \epsilon) = [d_4 \beta^2 + 3(d_7 \bar{e} + d_4 \epsilon) \beta + (d_8 \bar{e}^2 + 4d_7 \bar{e} \epsilon + 2d_4 \epsilon^2 + d_3)] \frac{\beta}{d_5} \quad (41)$$

with:

$$d_7 = d_2 - \frac{d_4}{d_5} = 3(1 + 2\mu \kappa n \mu - \mu^2) \frac{d_1}{d_5}$$

$$d_8 = d_6 - \frac{2}{d_5} (d_2 + d_7)$$

Note that for $0 < \mu < 1$, all the coefficients ($d_1 \dots d_8$) are greater than zero.

When the "equivalent imperfection" \bar{e} vanishes, the equation reduces to a bifurcation problem with the two branches

$$\beta = 0 \quad (\text{prebuckling})$$

and

$$\lambda = \frac{1}{d_5} (d_4 \beta^2 + 3d_7 \bar{e} \beta + d_8 \bar{e}^2 + d_3) \quad (\text{postbuckling}) \quad (42)$$

The "buckling load" λ'_{cr} is the intersection of the two lines and is given by:

$$\lambda'_{cr} = \frac{1}{d_5} (d_3 + d_8 \bar{e}^2) \quad (43)$$

The formula holds also for $\bar{e} = 0$ when it represents the "true" buckling load λ_{cr} of the corresponding centrally stiffened plate. It should be stressed again, though, that its validity is restricted to weakly stiffened plates. When the stiffener is relatively heavy, an additional term in the representation for ϕ is needed and the two parameter model would tend to exaggerate the buckling load.

When $\bar{e} \neq 0$, the postbuckling parabola crosses the $\beta=0$ axis at a positive slope. This implies that the buckling point is unstable and the load decreases for $\beta < 0$. The minimum of the parabola is reached at

$$\lambda_{min} = \lambda'_{cr} - \frac{9d_7^2}{4d_4 d_5} \bar{e}^2$$

This value of λ_{min} is higher than the critical loading λ_{cr} of the corresponding centric plate, indicating that for small eccentricities the degree of sensitivity of the postbuckling behavior is not very severe.

The behavior of the imperfect plate ($\epsilon \neq 0$) is best visualized by using the auxiliary variable $\gamma = (\beta + \epsilon)$. The equation for λ becomes then:

$$d_5 \lambda = d_4 \gamma^2 + 3d_7 \bar{e} \gamma + [d_5 \lambda'_{cr} - (d_4 \epsilon + 2d_7 \bar{e}) \epsilon] - (d_5 \lambda'_{cr} + d_7 \bar{e} \epsilon) \frac{\epsilon}{\gamma}$$

The additional effects of the imperfection are seen to be as follows:

- (i) A hyperbola which is mainly proportional to ϵ is added to the bifurcation parabola.
- (ii) The λ coordinate axis shifts ϵ units to the right
- (iii) The parabola translates downward by an amount which is essentially proportional to ϵ

Of the three, the last one is the least important and may be omitted for sufficiently small ϵ . Indeed, for sufficiently small ϵ the approximation which preserves all the important features is:

$$\lambda = \lambda'_{cr} (1 - \epsilon/\gamma) + \frac{1}{d_5} (d_4 \gamma^2 + 3d_7 \bar{e} \gamma)$$

Figure 3 presents the equilibrium paths for a plate with the following properties (corresponding to a plate for which test data is available):

$$\mu = 0.5; \bar{A} = 0.179; \bar{I} = 0.694; \bar{e} = 0.2$$

For this plate: $\lambda_{cr} = 4.281$. Also:

$$\lambda'_{cr} = 9.408$$

$$\lambda_{min} = 8.616$$

The equilibrium paths are shown in the figure for the following imperfections: $\epsilon = 0.2(\bar{\phi}_0 = -0.51)$; $\epsilon = 0(\bar{\phi}_0 = -0.71)$; $\epsilon = -0.01(\bar{\phi}_0 = -0.72)$;

$\epsilon = -0.1$ ($\bar{\phi}_0 = -0.81$). The bifurcation-type behavior for $\epsilon = 0$ and the post-buckling unstable behavior for $\epsilon = -0.01$ are clearly seen. For the other imperfections the equilibrium paths are stable over the entire range.

Several annular plates having similar configurations were tested in the past few years [8,10,11]. The results of the tests show a behavior which is very similar to the results given here. In addition, in some of the tests jump phenomena occurred with sudden changes in the measured rotations and subsequent stable behavior. This jump is very well modeled by the interaction analysis presented here.

10. SUMMARY OF RESULTS

(1) The capabilities and potentialities of semi-inextensional plate and shell models were demonstrated in the following:

(a) Development of the ordinary differential equation for the semi-inextensional axisymmetric deformations of shells of revolution.

(b) Comparison of an approximate semi-inextensional model for the annular plate with a corresponding (but more complex) extensional model.

(2) A study of the interactions between stiffener eccentricities and surface imperfections was initiated using simple models of the annular plate.

(a) The appearance of unstable postbuckling behavior and sensitivity was noted and examined. The sensitivity and its corresponding jump were restricted to a selected range of the parameters

and was limited in magnitude. It is possible that many "small scale" jump phenomenae which occur in tested stiffened structures are of this type. As demonstrated here, these need not be dangerous but their occurrence should be taken into consideration.

(b) The basic formulas for a more detailed study using a more complex model were developed and presented in a manner which is suitable for analysis (see Appendix).

APPENDIX: Equations for a Three-Parameter Semi-Inextensional Model

By introducing an additional rotational degree of freedom into the semi-inextensional model, its capabilities can be greatly increased so that even plates with smaller central openings ($0 < \mu < 1$) or heavier rotational edge restraints ($\bar{1} = 0(1)$ and higher) can be successfully treated and greater accuracy can be achieved. The penalty is in the increased amount of algebraic complexity. The basic equations are developed here and brought to a form which can be treated by simple algebraic means.

The question as to whether it is worthwhile to investigate this approach further, or to utilize existing nonlinear programs (such as BOSOR 5) instead, is left open.

The model is defined by the two angular parameters ($\phi_1; \phi_2$) in the expression for the rotation

$$\phi = \phi_1 + \phi_2(r/a)$$

and by the displacement u_b of the inner edge of the plate. Using (29), (7), (8b), the expressions for the strain measures are:

$$\epsilon_r = 0$$

$$\epsilon_\theta = \frac{a}{2r} \left[2 \frac{u_b}{a} + \frac{1}{3} \mu^3 \phi_2^2 + \mu^2 \phi_1 \phi_2 + \mu (\phi_1^2 - \phi_0^2) \right] - \frac{1}{6} \left(\frac{r}{a} \right)^2 \phi_2^2 - \frac{1}{2} \phi_1 \phi_2 \left(\frac{r}{a} \right) - \frac{1}{2} (\phi_1^2 - \phi_0^2)$$

$$K_r = \phi_2/a$$

$$K_\theta = \frac{1}{a} \phi_2 + \frac{1}{r} (\phi_1 - \phi_0)$$

Introducing into equation (31) for the total potential and performing the required integrations, the following expression for the total potential V results:

$$\begin{aligned} \frac{1}{\pi} V = & a^2 C \left\{ \frac{1}{216} (1-\mu^6) \phi_2^4 + \frac{1}{30} (1-\mu^5) \phi_2^3 \phi_1 + \frac{1}{48} (1-\mu^4) \phi_2^2 (5\phi_1^2 - 2\phi_0^2) + (1-\mu^3) \left[\frac{1}{6} \phi_2 \phi_1 (\phi_1^2 - \phi_0^2) - \right. \right. \\ & \left. \left. - \frac{1}{18} \phi_2^2 w \right] + \frac{1}{8} (1-\mu^2) [(\phi_1^2 - \phi_0^2)^2 - 2\phi_1 \phi_2 w] - \frac{1}{2} (1-\mu) (\phi_1^2 - \phi_0^2) w - w^2 \ln \mu \right\} + \\ & + D \left[(1+\nu) (1-\mu^2) \phi_2^2 + 2(1+\nu) (1-\mu) \phi_2 (\phi_1 - \phi_0) - (\phi_1 - \phi_0)^2 \ln \mu \right] + \\ & + \frac{1}{b} E \left\{ (1+\mu \phi_2 + \phi_1 - \phi_0)^2 + [u_b + (\mu \phi_2 + \phi_1 - \phi_0) e]^2 A \right\} - \\ & - a^2 P \left[\frac{1}{3} \phi_2^2 + \phi_2 \phi_1 + \phi_1^2 - \phi_0^2 - w \right] \end{aligned} \quad (A.2)$$

where:

$$w = 2 \frac{u_b}{a} + \frac{1}{3} \mu^3 \phi_2^2 + \mu^2 \phi_1 \phi_2 + \mu (\phi_1^2 - \phi_0^2)$$

The total potential can be now minimized with respect to the deformation parameters $(\phi_2; \phi_1; w)$. The results of this process lead, after some manipulations to the following three equations for the parameters in terms of the loading parameter λ and the geometry:

$$\begin{aligned} & \left(\frac{2}{5} A_5 - 4A_2 A_3 m \right) \bar{\phi}_2^3 + \left(\frac{5}{2} A_4 - 18A_2 m - 16A_1 A_3 m \right) \bar{\phi}_2^2 \bar{\phi}_1 + (2A_3 - 36A_1 A_2 m) \bar{\phi}_2 (\bar{\phi}_1^2 - \bar{\phi}_0^2) \\ & + (12\mu^3 \bar{A} - 72A_1 A_2 m) \bar{\phi}_2 \bar{\phi}_1^2 + (6A_2 - 144A_1^2 m) \bar{\phi}_1 (\bar{\phi}_1^2 - \bar{\phi}_0^2) + \left(6\frac{A_2}{A} \mu m + 16A_3 m - 16\mu^3 \right) \bar{\phi}_2^2 \\ & + 12 \left(\frac{2A_1 \mu m}{A} + 6A_2 m - 3\mu^2 \right) \bar{e} \bar{\phi}_2 \bar{\phi}_1 + 6 \left(\frac{A_2 m}{A} - 2\mu^2 \right) \bar{e} \bar{\phi}_2 (\bar{\phi}_1 - \bar{\phi}_0) + 12(A_1 m - \mu) \bar{e} (\bar{\phi}_1^2 - \bar{\phi}_0^2) + \\ & + 24 \left(\frac{A_1 m}{A} - \mu \right) \bar{e} \bar{\phi}_1 (\bar{\phi}_1 - \bar{\phi}_0) + 2[(1+\nu)(1-\mu) + \mu \bar{I}_c] \bar{\phi}_2 + 2(\bar{I}_c - \ln \mu) (\bar{\phi}_1 - \bar{\phi}_0) = [(1-6A_2 m) \bar{\phi}_2 \\ & + 2(1-12A_1 m) \bar{\phi}_1 + 24m \bar{e}] \lambda \end{aligned} \quad (A.3)$$

$$\begin{aligned}
 & \frac{2}{9}(A_6 - 8A_3^2 m) \bar{\phi}_2^3 + \frac{6}{5}(A_5 - 10A_2 A_3 m) \bar{\phi}_2^2 \bar{\phi}_1 + (A_4 - 16A_1 A_3 m) \bar{\phi}_2 (\bar{\phi}_1^2 - \bar{\phi}_0^2) + \frac{3}{2}(A_4 - 12A_2^2 m) \phi_2 \phi_1^2 + \\
 & + 2(A_3 - 18A_1 A_2 m) \bar{\phi}_1 (\bar{\phi}_1^2 - \bar{\phi}_0^2) + \left[\frac{8}{3} A_3 m \left(6 + \frac{1}{A} \right) - 6\mu^3 \right] \mu e \bar{\phi}_2^2 + 6 \left[A_2 m \left(12 + \frac{1}{A} \right) - 4\mu^2 \right] \mu e \bar{\phi}_2 \bar{\phi}_1 + \\
 & + 8 \left(\frac{mA_3}{3A} - \mu^3 \right) e \bar{\phi}_2 (\bar{\phi}_1 - \bar{\phi}_0) + 12(12mA_1 - \mu) \mu e (\bar{\phi}_1^2 - \bar{\phi}_0^2) + 6 \left(\frac{mA_2}{A} - 2\mu^2 \right) e \bar{\phi}_1 (\bar{\phi}_1 - \bar{\phi}_0) + \\
 & + 2 \left[(1+\nu)(1-\mu^2) + \mu^2 \bar{I}_c \right] \bar{\phi}_2 + 2 \left[(1+\nu)(1-\mu) + \mu \bar{I}_c \right] (\bar{\phi}_1 - \bar{\phi}_0) = \left[\frac{2}{3}(1-4mA_3) \bar{\phi}_2 + \right. \\
 & \left. (1-mA_2) \bar{\phi}_1 + 24\mu e \lambda \right] \quad (A.4)
 \end{aligned}$$

and:

$$\begin{aligned}
 -\bar{u}_b = m\lambda + \frac{1}{6}(\mu^3 - 4A_3 m) \bar{\phi}_2^2 + \frac{1}{2}(\mu^2 - 6A_2 m) \bar{\phi}_2 \bar{\phi}_1 + \frac{1}{2}(\mu - 12A_1 m) (\bar{\phi}_1^2 - \bar{\phi}_0^2) + \frac{m\mu e}{A} \bar{\phi}_2 + \\
 + \frac{m\mu e}{A} (\bar{\phi}_1 - \bar{\phi}_0) \quad (A.5)
 \end{aligned}$$

Here:

$$A_j = 1 - \nu^j (1-j\bar{\Lambda}) \quad (j = 1 \dots 6)$$

$$m = \frac{1}{12} (\bar{\Lambda} - 2n\mu)^{-1}$$

Also, I_c is the modified moment of inertia of the ring with respect to the midsurface of the plate, given by:

$$I_c = I + \Lambda e^2 (1-m)$$

Other notations are as in the previous chapters. For example:

$$\bar{I}_c = \frac{EI_c}{bD} \quad \phi_2 = \phi_2 a/h \quad \text{etc.}$$

Equations (A.3) and (A.4) have been derived by first taking $V, \bar{\phi}_1$ and $V, \bar{\phi}_2$ respectively, and then eliminating \bar{u}_b by using (A.5) which has been derived from V, w . In this fashion the rotational parameters are decoupled from \bar{u}_b and can be solved for separately. The general form of the equations is:

$$L_i(\bar{\phi}_2; \bar{\phi}_1) = \lambda M_i(\bar{\phi}_2; \bar{\phi}_1) \quad (i = 1, 2)$$

where L_i and M_i are cubic and linear operators, respectively, in $\bar{\phi}_2$ and $\bar{\phi}_1$. Hence, it is possible to eliminate λ from the equations and arrive at the single equation:

$$Q(\bar{\phi}_2; \bar{\phi}_1) = (L_2 M_1 - L_1 M_2)(\bar{\phi}_2; \bar{\phi}_1) = 0 \quad (A.6)$$

which describes the internal relationship between $\bar{\phi}_2$ and $\bar{\phi}_1$, irrespective of the loading. It is a quintic equation in $(\bar{\phi}_2; \bar{\phi}_1)$.

Using assumed values for $\bar{\phi}_1$ (starting from $\bar{\phi}_1 = \bar{\phi}_0$), the corresponding solutions for $\bar{\phi}_2$ can be found from (A.6) which becomes a fourth order polynomial in the $\bar{\phi}_2$ (the fundamental solution is the one starting from $\bar{\phi}_2 = 0$, but the other solutions can be useful for exploring additional equilibrium branches). For any pair of $(\bar{\phi}_1; \bar{\phi}_2)$ the loading can be found from (A.3). This yields the equilibrium path which can be represented as $\lambda = \lambda(\bar{\phi}_p)$ where $\bar{\phi}_p$ is the rotation at any convenient point in the plate. The only mathematical tool needed is the solution of a fourth order polynomial equation.

REFERENCES

1. Reissner, E. "On the Theory of Thin Elastic Shells." The H. Reissner Anniversary Volume, J.W. Edwards ed., 1949.
2. Wempner, G.A., "The Conical Disk Spring," Proc. U.S. Third Nat. Congr. Appl. Mech., pp. 473-478.
3. Schmidt, R. and Wempner, G.A., "The Nonlinear Conical Spring," ASME J. Appl. Mech., pp. 681-682, Dec. 1959.
4. Berger, H.M., "A New Approach to an Analysis of Large Deflections of Plates," ASME J. Appl. Mech., 22, p. 463, 1965.
5. McElman, I.A., Mikulas, M.M. Jr. and Stein, M., "Static and Dynamic Effects of Eccentric Stiffening of Plates and Cylindrical Shells," AIAA J., 4, pp. 887-894, 1966.
6. Berger, H.M., "On Von Karman's Equations and the Buckling of a Thin Elastic Plate," Comm. Pure and Appl. Math., 20, pp. 687-719, 1967.
7. Chi-Lung, Huang, "Post Buckling of an Annulus," AIAA J., 11, No. 12, Dec. 1973.
8. Rosen, A. and Libai, A., "Stability, Behaviour and Vibrations of an Annular Plate Under Uniform Compression," Technion, Dept. Aero. Eng., I.A.E. Rep. No. 229, 1974.
9. Chi-Lung, Huang, "On Postbuckling of Orthotropic Annular Plates," Int. J. Nonlin. Mech., 10, pp. 63-73, 1975.
10. Rosen, A. and Libai, A., "Stability and Behaviour of an Annular Plate Under Uniform Compression," Experimental Mechanics, 16, pp. 461-467, 1976.
11. Libai, A., Feder, M. and Rosen, A., "Quasilinear Behavior of Eccentrically Stiffened Compressed Annular Plates Near the Buckling Point," Israel J. Tech. 17, pp. 339-346, 1979.

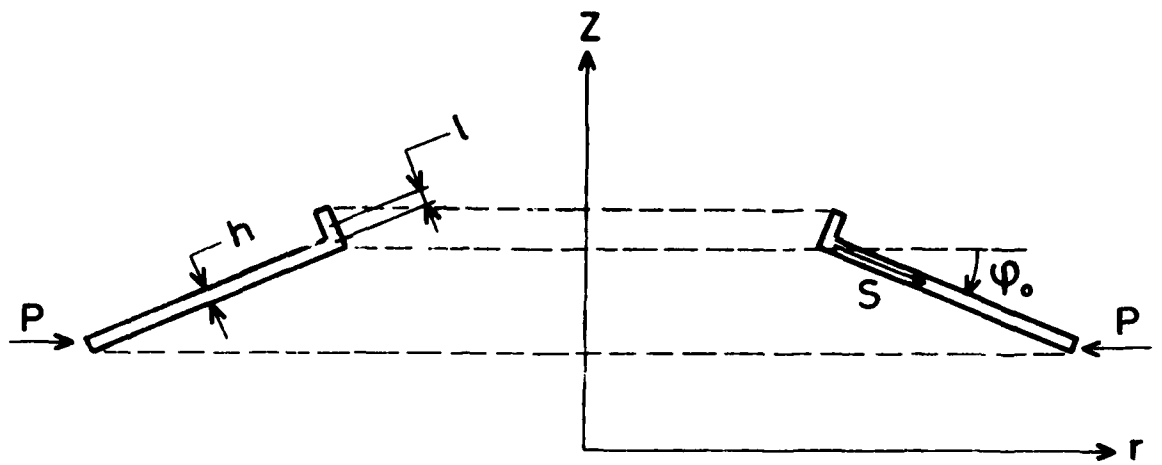
12. Tani, J., "Elastic Instability of an Annular Plate Under Uniform Compression and Lateral Pressure," ASME J. Appl. Mech., 47, 591-594, 1980.
13. Banerjee, B. and Datta, S., "A New Approach to an Analysis of Large Deflections of Thin Elastic Plates," Int. J. Nonlin. Mech. 16, pp. 47-52, 1981.
14. Libai, A. and Simmonds, J.G., "Large Strain Constitutive Laws for the Cylindrical Deformation of Shells," Int. J. Nonlin. Mech., 16, pp. 91-103, 1981.
15. Tani, J. and Yamaki, N., "Elastic Instability of a Uniformly Compressed Annular Plate with Axisymmetric Initial Deflection," Int. J. Nonlin. Mech., 16, pp. 213-220, 1981.

LIST OF FIGURES

Figure 1: Geometry of the Undeformed Annulus.

Figure 2: Deformation and Equilibrium.

Figure 3: Equilibrium Paths for an Eccentrically Stiffened Plate.



Cross section I-I and notations
 (ψ_0 is exaggerated for emphasis)

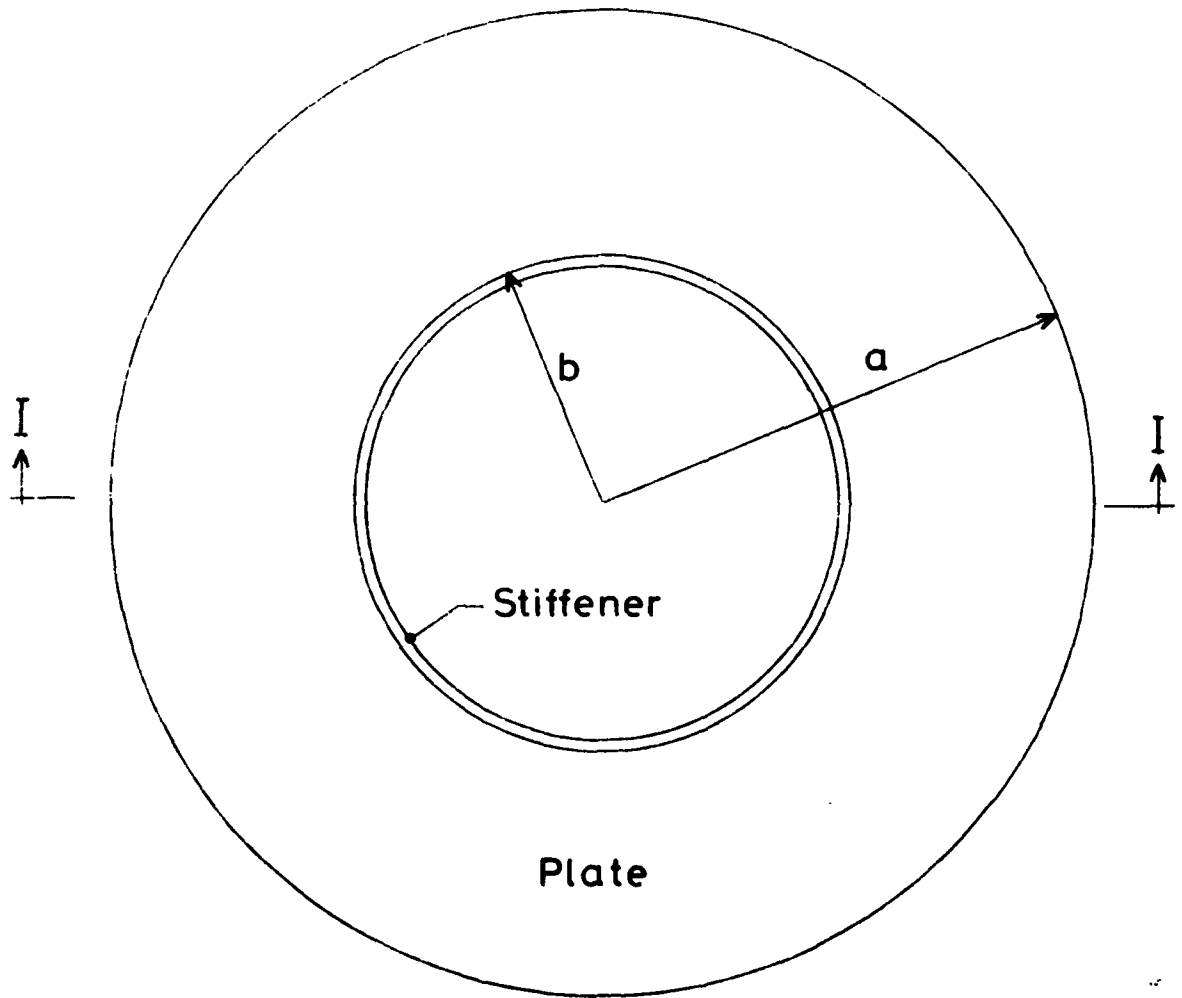


Figure 1: Geometry of the Undeformed Annulus.

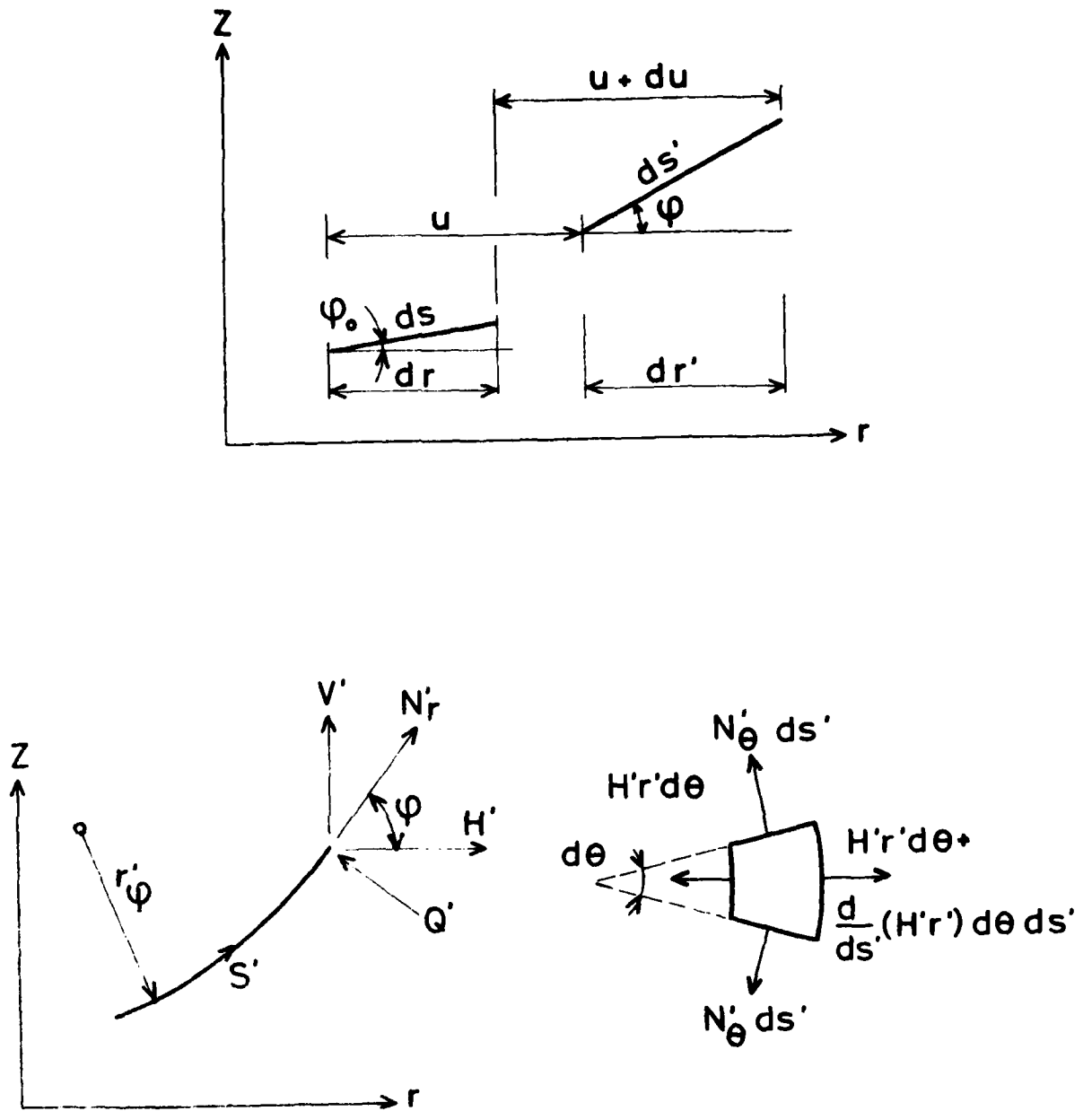


Figure 2: Deformation and Equilibrium.

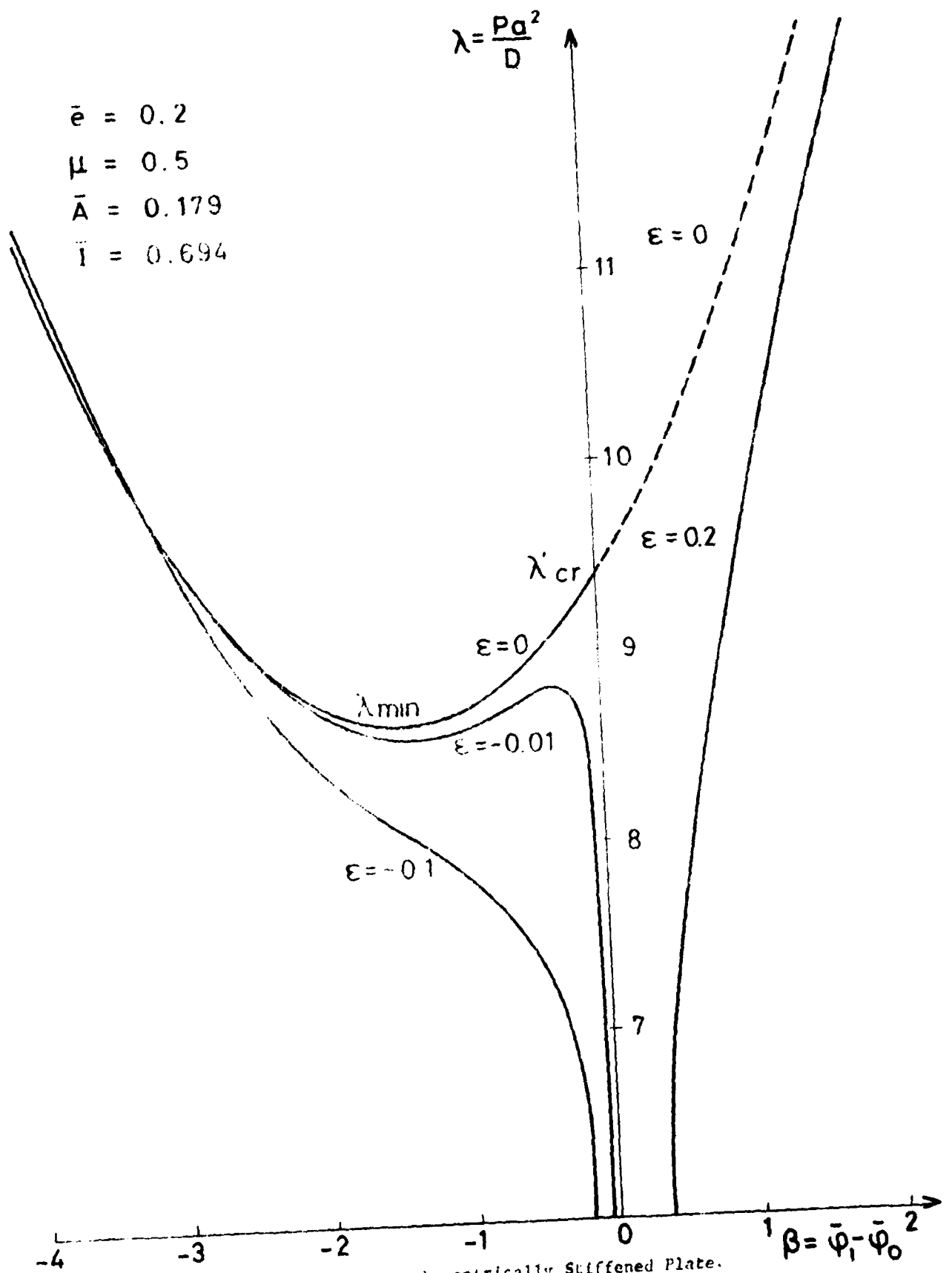


FIGURE 3: Equilibrium Paths for an Eccentrically Stiffened Plate.

**DAI
FILM**